Separation and Purification Technology 180 (2017) 107–113

Contents lists available at ScienceDirect

Separation and Purification Technology

journal homepage: www.elsevier.com/locate/seppur

Effects of roughness on droplet apparent contact angles on a fiber

M.M. Amrei [a], M. Davoudi [b], G.G. Chase [b], H. Vahedi Tafreshi [a,*]

[a] Department of Mechanical and Nuclear Engineering, Virginia Commonwealth University, Richmond, VA 23284-3015, USA
[b] Department of Chemical and Biomolecular Engineering, The University of Akron, Akron, OH 44325, USA

ARTICLE INFO

Article history:
Received 21 October 2016
Received in revised form 18 February 2017
Accepted 24 February 2017
Available online 27 February 2017

Keywords:
Droplet–fiber interactions
Droplet shape modeling
Surface roughness
Droplet contact angle

ABSTRACT

This paper reports on our investigation of the effects of surface roughness on the equilibrium shape and apparent contact angles of a droplet deposited on a fiber. In particular, the shape of a droplet on a roughened fiber is studied via the energy minimization method implemented in the surface evolver finite element code. Sinusoidal roughness varying in both the longitudinal and radial directions is considered in the simulations to study the effects of surface roughness on the most stable shape of a droplet on a fiber (corresponding a global minimum energy state). It is found that surface roughness delays droplet shape transition from a symmetric barrel to a clamshell or an asymmetric barrel profile. A phase diagram that includes the effects of fiber roughness on droplet configurations—symmetric barrel, clamshell, and asymmetric barrel—is presented for the first time. It is also found that droplet apparent contact angle tends to decrease on rough fibers. Likewise, roughness tends to increase the force required to detach a droplet from a fiber but the effect diminishes as droplet size increases relative to the size of surface roughness. The results presented in our study have been compared with experimental data or those from prior studies whenever possible, and good agreement has been observed.

1. Introduction

Understanding the interactions between a droplet and a fiber is of great importance to many applications. These applications include, but are not limited to, droplet filtration/separation, spray coating, electronic cooling, health and safety, fog harvesting, protective clothing, and medicine [1–6]. A simple manifestation of this effect in nature is the dew formation on spider webs or cactus spines, where life relies on the interactions between a droplet and a fiber in arid climate. Droplet–fiber interactions have been studied in many pioneering studies, and it has been shown that the Apparent Contact Angle (ACA) θ_{app} of a droplet with a fiber can be quite different from the Young–Laplace Contact Angle (YLCA) obtained for a small droplet of the same liquid deposited on a flat surface made from the same material [1–6]. Depending on fiber diameter, fiber surface energy, droplet volume, and droplet surface tension, two different conformations have been observed for a droplet deposited on a fiber. The first conformation, the barrel shape, tends to occur for larger droplets (relative to fiber), or for when the YLCA is relatively small. The second conformation, the clamshell, is mostly observed with small droplets, or when the YLCA is relatively high. In the former conformation, the droplet wets the fiber symmetrically while in the latter, the fiber is wetted on one side only. There are also droplet–fiber combinations where both of these conformations can be observed [4–11].

Roughness has been shown to affect the wettability of a surface. Wenzel proposed a relationship between YLCA θ_{YL} and the ACA of a droplet on a rough flat surface as $\cos\theta_{app} = r\cos\theta_{YL}$ where r is the ratio of the actual to the projected area of the rough surface [12]. However, the measured contact angles may not always match the predictions of this simple equation (see e.g., [13–19]). The knowledge gap is even wider when it comes to droplet contact angle on rough fibers (see e.g., [20–24]), and this has served as the motivation for undertaking the work presented here.

The remainder of this paper is structured as follows. First, we introduce our rough fiber equation and discuss the numerical modeling approach used to simulate the 3-D shape of a droplet on such a fiber (Section 2). We then present a validation study where we compare the predictions of our numerical simulations with the experiment for a few simple configurations in Section 3. Our investigations of the effects of surface roughness, fiber diameter, and droplet volume on the shape and ACAs of a droplet deposited are

Abbreviations: ACA, Apparent Contact Angle; PP, Polypropylene; PG, Propylene Glycol; SE, Surface Evolver; ULSD, Ultra Low Sulfur Diesel; YLCA, Young–Laplace Contact Angle.

* Corresponding author.
E-mail address: htafreshi@vcu.edu (H.V. Tafreshi).
URL: http://www.people.vcu.edu/~htafreshi/ (H.V. Tafreshi).

http://dx.doi.org/10.1016/j.seppur.2017.02.049
1383-5866/

reported in Section 4. In this section, we also study the transverse forces required to detach a droplet from a rough fiber for different droplet–fiber configurations. Finally, the conclusions drawn from the work are given in Section 5.

2. Numerical simulations

The surface energy minimization method implemented in the Surface Evolver (SE) finite element code is used to simulate the 3-D shape of a droplet deposited on a rough fiber. SE has shown to be accurate in predicting the air–water interface stability (see e.g., [25–28]). In this section, we first present the equations for producing a fiber having an arbitrary 3-D roughness, and then derive an equation for the energy of a droplet deposited on such a fiber. To our knowledge, no study has yet simulated or quantified roughness on a fiber using a mathematical function. Although real roughness is random in shape and arrangement, we considered sinusoidal roughness for the sake of simplicity (sinusoidal functions have also been used to model roughness on a flat surface [17,29]). A rose function (a sinusoid in polar coordinates) can generate sinusoidal roughness at each cross-section of the fiber [30]. By multiplying that equation by another sinusoidal function for

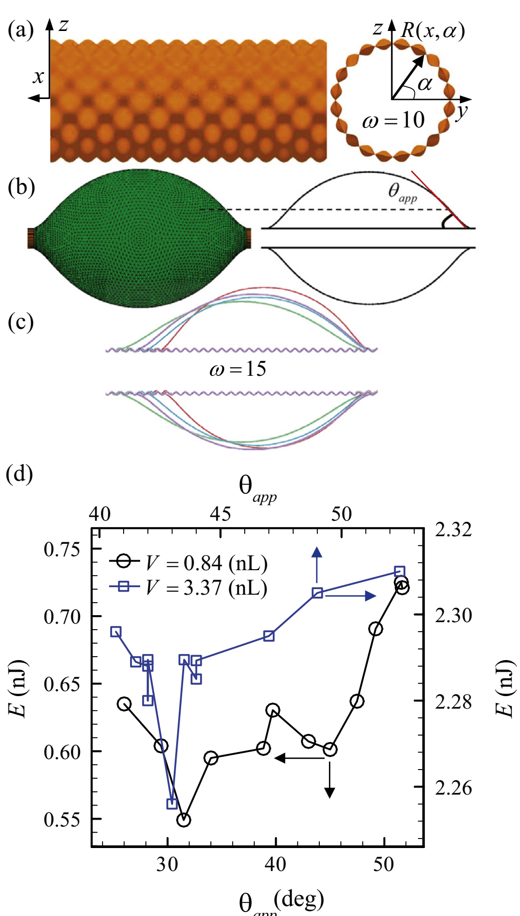

Fig. 1. Side and cross-sectional views of our virtual rough fiber is shown in (a). The inflection point and apparent contact angle are shown in (b). Overlaid images of droplet profiles corresponding to different local minimum energies are shown in (c) for a droplet with a volume of $V = 0.84$ nL on a rough fiber with $r_f = 15$ µm, $\theta_{YL} = 30°$ and $\omega = 15$. Droplet surface energy is plotted versus apparent contact angle in (d) for droplet volumes of $V = 0.84$ nL (black symbols) and $V = 3.37$ nL (blue symbols). (For interpretation of the references to colour in this figure legend, the reader is referred to the web version of this article.)

the direction along the fiber axis, we obtain a 3-D roughness for a fiber as shown in Fig. 1a.

Consider a fiber in the x-direction with a sinusoidal roughness in the axial and preferential directions, described as

$$R(x,\alpha) - r_f\left[1 + a\sin\left(\frac{2\pi}{\lambda r_f}x\right)\sin(\omega\alpha)\right] = 0 \tag{1}$$

where r_f is the smooth fiber radius, $R(x,\alpha) = \sqrt{y^2+z^2}$ is the local radius of the rough fiber at any point, and $\alpha = \mathrm{Arctan}\frac{z}{y}$ is angular position. In this equation, a is roughness amplitude, λ is roughness wavelength, and $\omega = \frac{2\pi}{\lambda}$ is the angular frequency of the roughness peaks (see Fig. 1a). For the sake of convenience, we define dimensionless roughness amplitude as $= \frac{a}{r_f}$ (note that $b = a$ if $r_f = 1$). SE is used here to obtain the equilibrium 3-D shape of a droplet deposited on a rough fiber by minimizing the total energy of the droplet–fiber system. For a single-droplet–single-fiber system, the total free energy E can be written as

$$E = \sigma_{LG}A_{LG} - \sigma_{LG}\int_{A_{SL}}\cos\theta_{YL}dA + \int\rho hgdV \tag{2}$$

where σ_{LG} is the surface tension of the liquid and A_{LG} and A_{SL} are liquid–gas and solid–liquid areas, respectively. Here, h represents the vectorial change in the droplet's centroid position caused by body forces (zero in the absence of external forces), g stands for the body force per unit mass, ρ represents the liquid density, and dA and dV are area and volume elements, respectively.

Our simulations start by placing a droplet with an arbitrary shape, but a fixed volume V, over the fiber and allowing it to evolve to an equilibrium shape and position while maintaining a fixed YLCA at the three-phase contact line. The surface evolver program evolves the droplet shape via a gradient descent method toward a minimal energy. In each iteration the contact line slips smoothly over the bumps in a way that energy of the system decreases until an equilibrium state is reached. A constraint was placed on the fiber surface to prevent any portion of the droplet body to overlap with the solid fiber (as the alternative would be non-physical). Therefore, there would only remain certain areas of a valley between two roughness peaks that a droplet contact line could reside at equilibrium. It is also important to note that solution convergence in these simulations depends more on the mesh density long the contact line than it depends on the total number of mesh used for the simulation. Convergence can often be achieved with a coarse mesh when the fiber is smooth. However, for a rough fiber an adaptive (dense) mesh near the contact line may become necessary to capture the surface roughness. We used a mesh size equal to $\frac{\lambda}{12}$ along the contact line for rough fibers.

We also calculated the mean curvature of the droplet at each point on the droplet surface (same at all points) for a few cases, and used it in the Laplace equation to obtain the droplet pressure. This pressure was then compared with that calculated by SE for further validation and very good agreement was observed.

The tangent to the inflection point of a droplet profile on a fiber has been considered as the ACA of the droplet in this work (see Fig. 1b). While we initially determined the ACAs by fitting a curve into digitized profiles of each droplet to find the inflection point (where the second derivative of the profile goes to zero), we later realized that similar ACAs can be measured from a computer screen by naked eyes (with an average margin of error of about 3°). The latter was considered in our work for its convenience.

As it has been discussed in the literature, there are an infinite number of ACAs (each corresponding to a local minimum energy) that a droplet can exhibit on a rough surface while depending on the position of its contact line on the surface asperities [13–19]. Fig. 1c shows examples of droplet profiles that can be observed